JOURNAL OF GUIDANCE, CONTROL, AND DYNAMICS
Vol. 23, No. 1, January–February 2000

Singular Arcs During Aerocruise

Lorenzo Casalino*
Politecnico di Torino, 10129 Torino, Italy

An indirect method is applied to the optimization of aeroassisted plane-change maneuvers; the theory of optimal control is used to find the control law that minimizes the propellant requirements. The switching function, which rules the use of thrust, is analyzed to find the optimal strategy. In the case of aeroglide maneuvers, which perform a nonpropelled atmospheric flight, the results show that the trajectory is often suboptimal. The final mass can be increased by performing an aerocruise maneuver, requiring the use of thrust inside the atmosphere. The use of an intermediate thrust level is the optimal strategy during this phase; the optimal control law for the thrust magnitude during this singular arc is derived, and the optimal trajectory is found numerically. Aerocruise trajectories with a singular arc are optimal in terms of propellant expenditure and present the additional benefit that thermal and dynamic loads are remarkably reduced relative to aeroglide maneuvers and are comparable to the loads of other aerocruise concepts.

Introduction

LOW cost in space transportation is one of the keys to human exploration and exploitation of space; aeroassisted transfers, which use aerodynamic forces in synergy with propulsive forces, are a promising means to perform several classes of orbit transfers, as they can allow great propellant savings relative to all-propulsive transfers.[1] Since the pioneering work by London,[2] a large number of studies[3] can be found in the literature, and only some indicative references are given in the present paper.

One of the most interesting applications of aeroassisted transfers is the plane-change of an Earth orbit (synergetic plane change). A distinction is made between two different strategies. Aeroglide maneuvers exclude the use of thrust inside the Earth's atmosphere; as a quick turn is more efficient, the vehicle has to penetrate deeply inside the atmosphere, thus producing high thermal and dynamic loads. On the contrary, aerocruise maneuvers use thrust inside the atmosphere and were originally proposed with the main objective of reducing dynamic and thermal loads.

Even in the simplest case of aeroglide maneuvers, the problem is complex, from a numerical point of view; the atmospheric portion of the flight is generally considered separately[4] (and eventually coupled to the space portion[5]) or approximate analyses, based on matched asymptotic expansions,[6] are conducted. In a previous paper[7] the author applied optimal control theory (OCT) to aeroglide maneuvers with a particular indirect technique that allows one to reduce the necessary simplifying assumptions. The switching structure was assigned, and the whole trajectory was split into arcs with given control strategies; the optimal controls during each arc and the boundary conditions at the arc junctions were derived. The boundary-value problem arising from the application of OCT was solved by means of a procedure based on Newton's method.[8] In particular, the thrust magnitude was ruled by the switching function, in agreement with Pontryagin's Maximum Principle; the analysis of the results of the paper showed that, in certain cases [in particular for transfers between Low Earth Orbits (LEOs)], the switching structure was not optimal and performance could be improved by using thrust inside the atmosphere, i.e., with an aerocruise maneuver.

In the present paper the same optimization procedure is applied to aerocruise transfers, while taking into account the requirements of Pontryagin's Maximum Principle and modifying the switching structure accordingly. This kind of mission has frequently been considered in the literature, but attention was mainly directed to the reduction of thermal loads. Theoretical and numerical difficulties were overcome by means of simplifying assumptions concerning the control strategy during the atmospheric pass. Several suboptimal strategies have been proposed: flight at constant altitude and velocity[9] (i.e., with constant thermal load), flight at constant altitude only,[10] and flight with thrust to cancel drag.[11] Attention is here directed toward propellant usage, and no constraint on the flight profile is imposed; the trajectory that maximizes the vehicle final mass is sought. For this purpose an intermediate thrust arc (singular arc) is necessary during the atmospheric flight. Singular arcs have already been considered for aeroassisted transfers; the necessity of a singular arc has been found when a constant altitude cruise, with thrust parallel to the vehicle velocity, is performed.[10] More recently, Ross[12] has presented the necessary conditions for the optimality of a singular arc in the case of flight with thrust parallel to the velocity, whereas no constraint was imposed on the altitude. In the present paper a new kind of aerocruise trajectory is considered. Both altitude and thrust direction are free; the optimal control law for the thrust magnitude during the atmospheric pass and the necessary conditions for the optimality of an aeroassisted transfer that includes a singular arc are derived. A numerical example for a plane change maneuver is presented to illustrate the characteristics of this new class of mission. A comparison with different aeroassisted trajectories is also shown to highlight the benefits that can be obtained by using thrust inside the atmosphere.

Statement of the Problem

The aeroassisted plane-change transfer between two orbits with the same radius is considered in the present paper. The vehicle is assumed to be a point mass with varying mass m; the vehicle motion is described by the position and velocity vectors ($\boldsymbol{r}$ and $\boldsymbol{v}$, respectively) in an inertial frame, with the origin at Earth's center. The vehicle is subject to the gravitational field $\boldsymbol{g}$, thrust $\boldsymbol{T}$, lift $\boldsymbol{L}$, and drag $\boldsymbol{D}$; the equations of motion are

$$\dot{\boldsymbol{r}} = \boldsymbol{v} \tag{1}$$

$$\dot{\boldsymbol{v}} = \boldsymbol{g} + \boldsymbol{T}/m + \boldsymbol{D}/m + \boldsymbol{L}/m \tag{2}$$

$$\dot{m} = -T/c \tag{3}$$

where c is the effective exhaust velocity, considered to be constant. As Earth's rotation is taken into account, aerodynamic forces depend on the relative velocity $\boldsymbol{v}_{\text{rel}} = \boldsymbol{v} - \boldsymbol{\omega} \times \boldsymbol{r}$, where $\boldsymbol{\omega}$ is Earth's angular velocity vector. To carry out the integration, the equations of motion are represented in a suitable reference frame.[13] The position vector is described by radius, longitude, and latitude in an inertial frame based in the equatorial plane. The inertial velocity is expressed in a topocentric reference frame by means of components in the zenith (i.e., radial), east, and north directions. All variables have been made

Received 29 October 1998; revision received 28 June 1999; accepted for publication 26 July 1999. Copyright © 1999 by the American Institute of Aeronautics and Astronautics, Inc. All rights reserved.

*Researcher, Dipartimento di Energetica, Corso Duca degli Abruzzi, 24. Member AIAA.

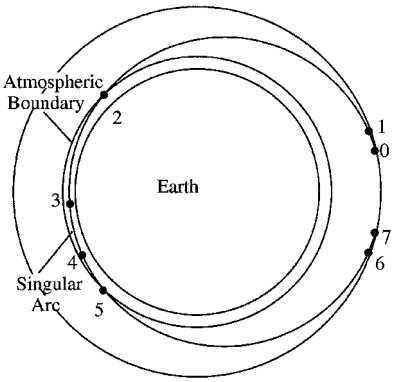

Fig. 1 Sketch of the aerocruise maneuver.

nondimensional by using Earth's mean radius (6371 km), the corresponding circular velocity (7.91 km/s), and the vehicle initial mass m_0 as reference values.

The trajectory is controlled by propulsion (i.e., by thrust magnitude and direction) and by aerodynamic forces. By introducing the dynamic pressure $q = 0.5\rho v_{\text{rel}}^2$ (ρ is the air density), the reference surface area S, and two nondimensional coefficients, the magnitude of lift and drag are expressed as $L = qSC_L$ and $D = qSC_D$, respectively. If the drag polar of the vehicle $C_D = C_D(C_L)$ is assigned, lift and drag magnitude are controlled only by the lift coefficient C_L. The lift direction is controlled by banking the vehicle around the relative velocity; the bank angle σ is the angle between the lift vector and the $(\boldsymbol{r}, \boldsymbol{v}_{\text{rel}})$ plane; it is positive if the vehicle is banked to the left. Five control variables are used: the thrust magnitude and two thrust angles (elevation and azimuth) to determine the thrust, the lift coefficient and the bank angle to determine the aerodynamic forces.

The procedure optimizes the trajectory, i.e., determines the controls to maximize the final mass (the initial mass is unity); the atmospheric pass is not separately considered, but the space and atmospheric portions of the trajectory are simultaneously optimized. A rather peculiar approach to the problem is adopted; the trajectory is divided into arcs by assuming its switching structure, i.e., a suitable succession of phases with assigned control strategies; the switching structure is then checked in light of Pontryagin's Maximum Principle.

The aerocruise maneuver has been sketched (not to scale and in the same plane) in Fig. 1. Each jth phase starts at point $j-1$ and ends at point j. The optimal thrust magnitude and direction are used during every propelled phase. During the initial deorbit phase, thrust is used to reduce the periapsis in order to transfer the vehicle into an orbit that intercepts the Earth's atmosphere; a partial rotation of the orbit plane is also performed in this phase. After a coast arc (phase 2) the vehicle crosses the atmospheric boundary at point 2, and atmospheric flight with optimal lift coefficient and direction (phases 3, 4, and 5) follows. Phases 3 and 5 are nonpropelled, and lift is banked in order to obtain a lift component out of the trajectory plane that changes the orbit inclination, whereas the in-plane component controls the flight altitude. These phases are joined by the cruise phase, where thrust is used to recover the energy depletion caused by drag but also (together with lift) to change the orbit plane and control the altitude. A coast arc (phase 6) follows the exit from the atmosphere, and then the propelled reorbit phase (7) inserts the vehicle into the final orbit; the rotation of the orbit plane up to the required inclination is performed in this phase.

The problem is completed by the boundary conditions, which are the same as in the case of aeroglide maneuvers. At the initial and final points ($j = 0, 7$) the magnitudes of radius and velocity [$r_j = R$ and $v_j = \sqrt{(1/R)}$] are assigned; for circular orbits $\boldsymbol{r}_j^T \boldsymbol{v}_j = 0$; the inclination i_j is assigned by posing $\boldsymbol{Z} \cdot (\boldsymbol{r}_j \times \boldsymbol{v}_j) = |\boldsymbol{r}_j \times \boldsymbol{v}_j| \cos i_j$ where $\boldsymbol{Z}$ is a unit vector parallel to the Earth axis; moreover, $m_0 = 1$ and $t_0 = 0$ at the initial point. The radius magnitude is also imposed at the atmospheric boundaries ($j = 2, 5$) $r_j = r_a$.

The propelled phases can also be modeled as impulsive maneuvers; in this case, a discontinuity in the state variables takes the place of the finite-thrust arc ($j = 0, 6$): $\boldsymbol{v}_{j+1} = \boldsymbol{v}_j + \Delta\boldsymbol{v}$ and $m_{j+1} = m_j \exp(-\Delta v/c)$.

Optimization

To exploit OCT, an adjoint variable is associated to each differential equation, and the Hamiltonian is defined as

$$H = \lambda_r^T \boldsymbol{v} + \lambda_v^T \boldsymbol{g} + (T/m) S_F + (qS/m) A_F \tag{4}$$

The thrust acceleration coefficient

$$S_F = \lambda_v^T \boldsymbol{T}/T - \lambda_m m/c \tag{5}$$

is usually called the switching function; a similar coefficient

$$A_F = -C_D \lambda_v^T \boldsymbol{v}_{\text{rel}}/v_{\text{rel}} + C_L \lambda_v^T \boldsymbol{L}/L \tag{6}$$

is associated with the aerodynamic acceleration.

The time derivatives of the adjoint variables are given by the Euler–Lagrange equations

$$\dot{\lambda}_r^T = -\frac{\partial H}{\partial \boldsymbol{r}} = -\lambda_v^T [G] - \frac{S}{m}\left(A_F \frac{\partial q}{\partial \boldsymbol{r}} + q \frac{\partial A_F}{\partial \boldsymbol{r}}\right) \tag{7}$$

$$\dot{\lambda}_v^T = -\frac{\partial H}{\partial \boldsymbol{v}} = -\lambda_r^T - \frac{S}{m}\left(A_F \frac{\partial q}{\partial \boldsymbol{v}} + q \frac{\partial A_F}{\partial \boldsymbol{v}}\right) \tag{8}$$

$$\dot{\lambda}_m = -\frac{\partial H}{\partial m} = \lambda_v \frac{T}{m^2} + A_F \frac{qS}{m^2} \tag{9}$$

where $[G] = \partial \boldsymbol{g}/\partial \boldsymbol{r}$ is the gravity-gradient matrix.

According to Pontryagin's Maximum Principle, optimal controls maximize the Hamiltonian at each point of the trajectory. Equation (4) is maximized if the thrust direction is parallel to the velocity adjoint vector $\boldsymbol{\lambda}_v$, the primer vector,[14] which gives the thrust angles.[13] Equation (5) becomes

$$S_F = \lambda_v - \lambda_m m/c \tag{10}$$

The Hamiltonian is linear with respect to the thrust magnitude T; maximum and minimum (i.e., null) thrust arcs alternate according to the sign of S_F. Intermediate thrust arcs (singular arcs) might occur only if S_F is null during the whole arc, that is, if S_F and its time derivatives vanish. Maximum thrust is commonly used for deorbit and reorbit phases[4–6]; therefore, singular arcs are excluded during flight outside the atmosphere. As far as the cruise phase is concerned, the problem was first analyzed by supposing a maximum-thrust atmospheric flight; anomalies in the switching function behavior (that is, the solution violated Pontryagin's Maximum Principle) have suggested the introduction of a singular arc. The nullity of the switching function and its first time derivative $\dot{S}_F$ is enforced at the beginning of the singular arc ($j = 4$). The thrust magnitude appears explicitly in the second time derivative $\ddot{S}_F$, and the optimal thrust magnitude T^* can therefore be determined by nulling $\ddot{S}_F$ at each point of the singular arc, as shown in the Appendix.

The optimal lift direction is also determined by the primer; the Hamiltonian is maximized if lift is in the plane determined by the relative velocity and primer vectors.[15] The optimal bank angle can be explicitly obtained by posing $\partial H/\partial \sigma = 0$ once the equations have been represented in the aforementioned frames.[13] By introducing the angle δ between $\boldsymbol{V}_r$ and $\boldsymbol{\lambda}_v$, Eq. (6) takes the form

$$A_F = -C_D \lambda_v \cos\delta + C_L \lambda_v \sin\delta \tag{11}$$

The optimal lift coefficient is obtained by nulling the Hamiltonian partial derivative with respect to C_L, that is, by posing $\partial A_F/\partial C_L = 0$; one obtains

$$\frac{\partial C_D}{\partial C_L} = \tan\delta \tag{12}$$

A parabolic drag polar $C_D = C_{D0} + KC_L^2$ is assumed throughout, and the optimal lift coefficient becomes

$$C_L = \tan\delta/2K \tag{13}$$

The remaining boundary conditions are provided by OCT; according to the adopted switching structure, the optimum conditions

on the Hamiltonian and adjoint variables are obtained by means of an almost mechanical application[16] of general expressions that can be found in OCT textbooks.[17] At the initial and final point ($j = 0, 7$) one obtains

$$\frac{\lambda_{rj}^T \boldsymbol{v}_j}{\lambda_{vj}^T \boldsymbol{r}_j} = \frac{v_j^2}{r_j^2} \qquad \frac{\lambda_{rj}(\boldsymbol{r}_j \times \boldsymbol{v}_j)}{\lambda_{vj}(\boldsymbol{r}_j \times \boldsymbol{v}_j)} = \frac{v_j^2}{r_j^2}\frac{\boldsymbol{Z}^T \boldsymbol{r}_j}{\boldsymbol{Z}^T \boldsymbol{v}_j} \tag{14}$$

The Hamiltonian must be null at the final point and continuous at each internal point; these conditions are equivalent to nulling the switching function when the engine is turned on and off and state the continuity of the radius adjoint variable (which could be discontinuous) at the atmospheric boundary. As the final mass is maximized, $\lambda_{m7} = 1$ is also obtained at the final point. When an impulsive burn is considered, the adjoint variables are continuous but $\lambda_{mj+1} = \lambda_{mj} \exp(\Delta v / c)$. The nullity of the switching function at the extremities of the finite-thrust arc is substituted by the nullity of S_F and $\dot{S}_F$ at the impulse, which is parallel to the primer vector.[7]

The multipoint boundary-value problem is solved by means of a procedure[8] based on Newton's method and summarized here . The vector $\boldsymbol{x}$ includes state, adjoint variables, and unknown constant parameters (for instance, the time length of each phase). Once the optimal controls are derived as a function of $\boldsymbol{x}$, the differential equations reduces to $\dot{\boldsymbol{x}} = \boldsymbol{f}(\boldsymbol{x})$. The procedure searches for the initial value $\boldsymbol{x}_0$ that satisfies the boundary conditions $\chi(\boldsymbol{s}) = 0$, where $\boldsymbol{s}$ includes the variable values at all of the internal and external boundaries. The problem is solved iteratively; a tentative vector of the unknown initial values $\boldsymbol{x}_0 = \boldsymbol{p}$ is assumed, and the error χ is calculated. At each iteration $\boldsymbol{p}$ is modified according to the linearized relation

$$\Delta \boldsymbol{p} = -\left[\frac{\partial \chi}{\partial \boldsymbol{p}}\right]^{-1} \chi \tag{15}$$

to null the error on the boundary conditions; the matrix in Eq. (15) is computed as a product of two matrices

$$\left[\frac{\partial \chi}{\partial \boldsymbol{p}}\right] = \left[\frac{\partial \chi}{\partial \boldsymbol{s}}\right]\left[\frac{\partial \boldsymbol{s}}{\partial \boldsymbol{p}}\right] \tag{16}$$

The sensitivity of the boundary conditions with respect to the variable values at the boundaries $[\partial \chi / \partial \boldsymbol{s}]$ is obtained by simple derivation; the sensitivity of the variable values with respect to the initial values $[\partial \boldsymbol{s} / \partial \boldsymbol{p}]$ is given by the value (at the boundaries) of the matrix that is obtained by integrating the homogeneous system

$$\frac{\mathrm{d}}{\mathrm{d}t}\left[\frac{\partial \boldsymbol{x}}{\partial \boldsymbol{p}}\right] = \left[\frac{\partial \boldsymbol{f}}{\partial \boldsymbol{x}}\right]\left[\frac{\partial \boldsymbol{x}}{\partial \boldsymbol{p}}\right] \tag{17}$$

Numerical Example

Aeroassisted transfers can provide the highest benefit for plane-change transfers between LEOs. The transfer from a direct equatorial orbit, with radius $r = 1.1$, to a 30-deg inclined orbit, with the same radius, has been chosen to point out the characteristics of the aeroassisted transfer with a singular arc. The air density is approximated by dividing the atmosphere into five intervals starting from the Earth's surface (junction points occur at 25, 50, 75, and 100 km) and by assuming, for each ith interval, an exponential relation

$$\rho = \rho_i \exp(-a_i h^{b_i}) \tag{18}$$

in order to interpolate the U.S. Standard Atmosphere. The atmospheric boundary is fixed at $r_a = 1.02$; the aerodynamic forces are neglected at higher radii. Impulsive maneuvers, with the obvious exception of the finite-thrust singular arc, are assumed in the present example. Vehicle characteristics typical of aeroassisted transfers[4,18] are assumed and given in Table 1. For this maneuver the lift coefficient never exceeds the maximum value $C_{L\max}$; this constraint is not active, but it could be easily introduced[7] if required for lower orbit radii.

Figure 2 compares the switching function of the aeroglide and aerocruise maneuvers (full circles indicate impulses, and empty circles indicate the atmospheric boundary). The aeroglide transfer, which presents a reboost impulse at the exit from the atmosphere to recover the energy depletion caused by drag, is not optimal as S_F becomes positive during the nonpropelled atmospheric flight. On the contrary, the aerocruise maneuver with the singular arc, which occurs when $S_F = 0$, completely satisfies Pontryagin's Maximum Principle. Therefore, it provides the maximum final mass, as can be seen in Table 2, which compares the aeroglide and aerocruise transfers to the all-propulsive single-impulse maneuver for the same plane-change. Results corresponding to a maneuver with a cruise phase where thrust cancels drag exactly[19] are also shown. The final mass m_f of the aerocruise transfer is 9.3% higher compared to the aeroglide maneuver (and 62% higher if compared to the all-propulsive maneuver). However, one should also note the large decrease of dynamic and thermal loads; the maximum dynamic pressure $q_{\max}$ is 67.5% lower, whereas the maximum heat flux $h_{\max}$ for a 1-m radius sphere, which is usually taken as a reference value, is 42% lower (the heat flux h has been computed by using the relation[18] $h = 3.08 \times 10^{-4} \rho^{0.5} v_{\mathrm{rel}}^{3.08}$, where h is expressed in W/cm^2, the air density ρ in kg/km^3, and the relative velocity v_{rel} in km/s).

Table 1 Vehicle characteristics

Quantity	Value
Mass per unit surface (kg/m^2), m_0/S	300
Minimum drag coefficient, C_{D0}	0.1
Induced drag factor, K	1.1
Maximum lift coefficient, $C_{L\max}$	0.9
Effective exhaust velocity (m/s), c	2927

Table 2 Maneuver comparison

Mission strategy	m_f	$z_{\min}$, km	$q_{\max}$, kN/m^2	$h_{\max}$, W/cm^2
All propulsive	0.263	——	——	——
Aeroglide[7]	0.391	44.0	48.3	158.1
Thrust-drag cancellation[19]	0.394	45.3	39.7	139.7
Aerocruise	0.427	52.8	15.7	91.7

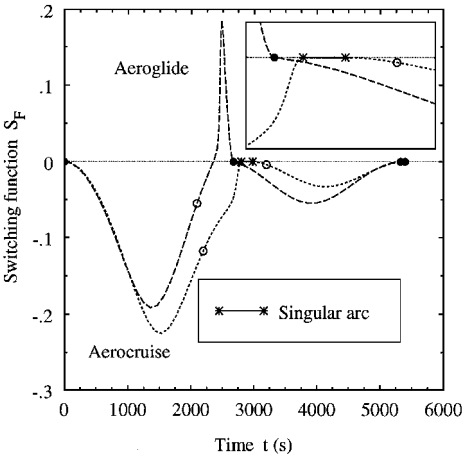

Fig. 2 Switching function comparison.

Figures 3 and 4 compare the bank angle and lift coefficient during the atmospheric flight (asterisks denote the extremities of the singular arc). Time lengths are quite different because in the aerocruise maneuver the vehicle follows a less steep trajectory (see also Fig. 5) and stays in the atmosphere longer. In the example the vehicle crosses the atmosphere while flying from south to north, and a positive bank angle increases the orbit inclination. For the aeroglide maneuver σ spans a larger range; during the initial phase of the flight, a lift component toward the Earth ($\sigma > 90$ deg) is used to take the vehicle to lower altitudes. Lift is then rotated outward ($\sigma < 90$ deg) to take the vehicle out of the atmosphere; for the same purpose, a high lift coefficient is required during this phase. On the contrary, during the aerocruise maneuver lift is more efficiently used; the bank angle remains closer to 90 deg (i.e., the value for which the whole lift is used to change the orbit plane), and C_L remains closer to the value corresponding to the maximum lift-to-drag

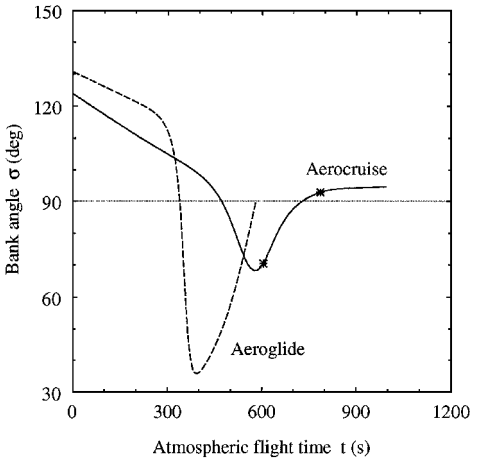

Fig. 3 Bank angle.

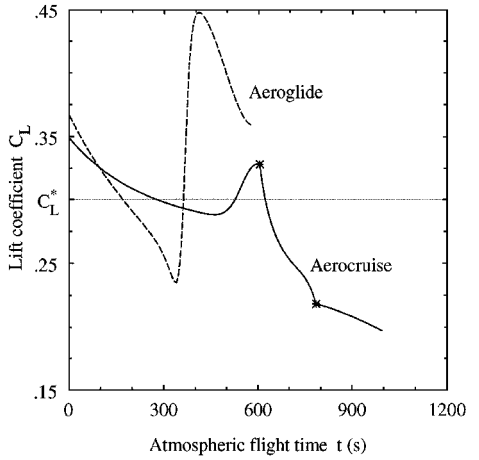

Fig. 4 Lift coefficient.

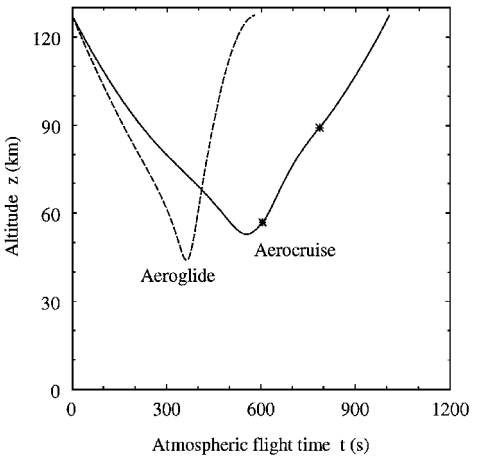

Fig. 5 Altitude.

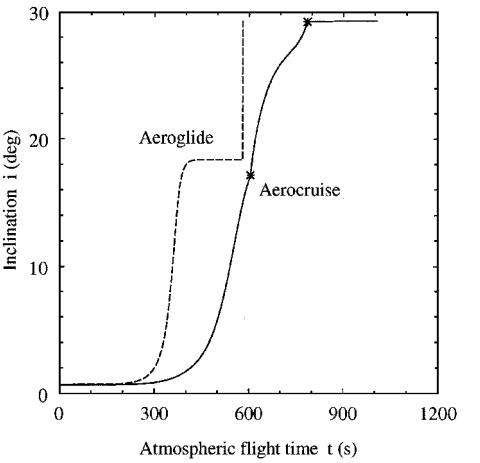

Fig. 6 Inclination.

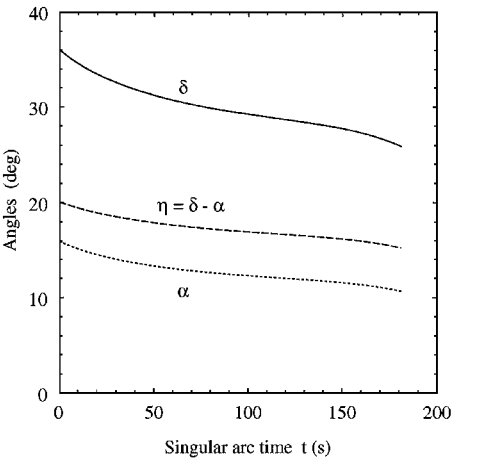

Fig. 7 Thrust-lift misalignment.

ratio C_L^*. Only during the final phase of the atmospheric flight does it decrease to lower values. A large outward component of lift is no longer necessary, as thrust can be used during the singular arc to take the vehicle out of the atmosphere. Controls are continuous at the singular arc extremities, whereas their time derivatives are discontinuous.

Figures 5 and 6 show the history of the altitude z and the inclination i, respectively, during the atmospheric flight. The rotation of the orbit plane is obtained in a similar way; at entry into the atmosphere, the orbit inclination, which is obtained during the deorbit phase, is about 0.7 deg. The curve slope progressively increases as the vehicle penetrates more deeply into the atmosphere, and lift becomes larger because of the higher air density; for the aeroglide maneuver the inclination at the atmosphere exit is 18.4 deg, and it increases up to 29.3 deg during the reboost phase. The aerocruise transfer presents similar features; a 17.2 deg orbit inclination is attained at the beginning of the singular arc, but the plane-change is obtained at higher altitudes by means of a more efficient use of the aerodynamic forces. The same plane change as in the reboost phase of an aeroglide maneuver is now obtained during the singular arc (the orbit inclination is 29.2 deg at its end and 29.3 deg at the atmosphere exit) when thrust and lift are synergetically used to change the orbit plane. The thrust contribution to the plane-change is highlighted by the increased slope of the inclination curve in Fig. 6. The singular arc occurs after the vehicle has attained the minimum altitude and when the maximum dynamic and thermal load have already been reached; therefore, they are not affected by the velocity increase because of the use of thrust.

The thrust direction is always parallel to the primer vector; thrust, lift, and relative velocity are therefore in the same plane. The angle δ between the thrust and relative velocity vectors is shown in Fig. 7, as a function of time during the singular arc. The angle δ is compared to the angle of attack α, measured from the zero-lift direction [a linear relation $C_L = C'_L \alpha$ has been assumed for the sake of simplicity; $C'_L = 0.0205(^\circ)^{-1}$ has been estimated according to data provided in the literature[9]]. The angle η, which is the difference between δ and α, represents the angle between the thrust and the zero-lift direction, which is fixed with respect to the vehicle; the small range between the maximum and minimum values that η assumes ($\Delta\eta = 20.09$ deg $- 15.22$ deg $= 4.87$ deg) represents the thrust-vectoring angle required to perform the present optimal aerocruise maneuver. The thrust component parallel to the relative velocity $T \cos\delta$, which recovers the energy depletion, is always dominant and increases, compared to the other components, as δ decreases.

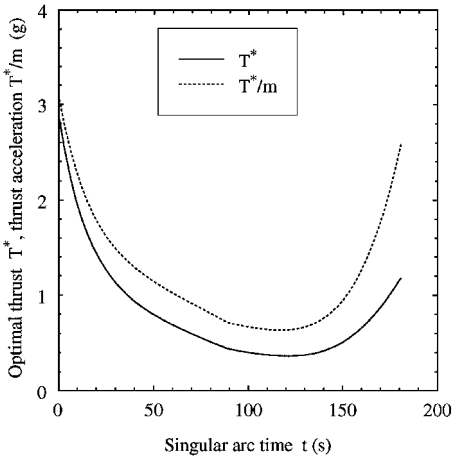

Fig. 8 Optimal thrust magnitude.

The component $T \sin\delta \sin\sigma$ is used to increase the orbit inclination, whereas $T \sin\delta \cos\sigma$ (always in the outward direction) takes the vehicle out of the atmosphere.

The use of thrust inside the atmosphere presents a twofold advantage. Propulsion is used at low altitudes, where the vehicle velocity is higher and the energy is increased more efficiently, and it allows a better control of the atmospheric flight compared to the aeroglide transfer. The necessity of controlling the altitude without the aid of the thrust imposes some constraints on the use of lift during the aeroglide manuever, thus diminishing its performance. The usefulness of the thrust magnitude control is illustrated in Fig. 8, which shows the optimal thrust T^* and the corresponding thrust acceleration T^*/m during the singular arc. High thrust is used in the initial phase to recover the energy depletion (with high efficiency because the vehicle is at low altitude) and to change the orbit plane (the vehicle is still in the proximity of the equator, where the plane change is efficient); then the thrust magnitude decreases to avoid excessive aerodynamic drag; finally it grows to higher values to complete the energy recovery when the air density is lower, because of the increased altitude.

Conclusions

An indirect method based on the theory of optimal control has been applied to aeroassisted plane-change transfers between LEOs to minimize the propellant requirements. An appropriate use of Pontryagin's Maximum Principle suggests when the use of thrust inside the atmosphere is required, an aerocruise maneuver must be performed; in this case the optimal strategy implies an intermediate thrust arc (singular arc) during the atmospheric flight; the corresponding control law has been derived and successfully applied. Results show that the aerocruise maneuver with a singular arc is not only optimal in terms of propellant expenditure, but also significantly reduces thermal and dynamic loads compared to aeroglide transfers by virtue of a more efficient use of lift, which allows one to obtain the required aerodynamic plane change at higher altitudes.

Appendix: Singular Arc

A vector formulation is adopted in the present Appendix; the scalar expressions are extremely long and tedious and have been omitted for the sake of conciseness. The first total derivative of the switching function for the present autonomous problem

$$\dot{S}_F = \frac{\partial S_F}{\partial \boldsymbol{x}}\dot{\boldsymbol{x}} + \frac{\partial S_F}{\partial \boldsymbol{\lambda}}\dot{\boldsymbol{\lambda}} \tag{A1}$$

is obtained by using Eqs. (3), (8), and (9):

$$\dot{S}_F = -\boldsymbol{\lambda}_r^T \boldsymbol{\lambda}_v / \lambda_v - (S/m)\left[q A_F/c + (A_F \boldsymbol{Q}_v^T + q\boldsymbol{A}_v^T)(\boldsymbol{\lambda}_v/\lambda_v)\right] \tag{A2}$$

where the vectors

$$\boldsymbol{Q}_v^T = \frac{\partial q}{\partial \boldsymbol{v}} \qquad \boldsymbol{A}_v^T = \frac{\partial A_F}{\partial \boldsymbol{v}} \tag{A3}$$

have been introduced; analogously, by carrying out the derivatives with respect to $\boldsymbol{r}$ and $\boldsymbol{\lambda}_v$, the vectors $\boldsymbol{Q}_r$, $\boldsymbol{A}_r$, and $\boldsymbol{A}_\lambda$ are defined.

The second derivative of the switching function can be similarly obtained:

$$\ddot{S}_F = \frac{\partial \dot{S}_F}{\partial \boldsymbol{x}}\dot{\boldsymbol{x}} + \frac{\partial \dot{S}_F}{\partial \boldsymbol{\lambda}}\dot{\boldsymbol{\lambda}} \tag{A4}$$

The velocity and mass time derivative depends on the thrust T, which therefore appears explicitly in the expression of $\ddot{S}_F$. By separating the gravitational and aerodynamic acceleration $\boldsymbol{a}_0$ from the thrust acceleration

$$\dot{\boldsymbol{v}} = \boldsymbol{a}_0 + \boldsymbol{T}/m \tag{A5}$$

and by introducing the matrices

$$[M_r] = A_F \frac{\partial \boldsymbol{Q}_v}{\partial \boldsymbol{r}} + q\frac{\partial \boldsymbol{A}_v}{\partial \boldsymbol{r}} \tag{A6}$$

$$[M_v] = A_F \frac{\partial \boldsymbol{Q}_v}{\partial \boldsymbol{v}} + q\frac{\partial \boldsymbol{A}_v}{\partial \boldsymbol{v}} \tag{A7}$$

$$[M_\lambda] = q\frac{\partial \boldsymbol{A}_v}{\partial \boldsymbol{\lambda}_v} \tag{A8}$$

and the scalar quantities

$$B_Q = \boldsymbol{Q}_v^T(\boldsymbol{\lambda}_v/\lambda_v) \qquad B_A = \boldsymbol{A}_v^T(\boldsymbol{\lambda}_v/\lambda_v) \tag{A9}$$

$$C_Q = B_Q + (q/c) \qquad C_A = B_A + A_F/c \tag{A10}$$

one obtains

$$\ddot{S}_F = \Lambda - (S/m)(\boldsymbol{S}_r^T\dot{\boldsymbol{r}} + \boldsymbol{S}_v^T\boldsymbol{a}_0 + \boldsymbol{S}_\lambda^T\boldsymbol{\lambda}_v + S_T T) \tag{A11}$$

where

$$\Lambda = -(\dot{\boldsymbol{\lambda}}_r^T/\boldsymbol{\lambda}_v)\boldsymbol{\lambda}_v - (\dot{\boldsymbol{\lambda}}_v^T/\boldsymbol{\lambda}_v)\left[\boldsymbol{\lambda}_r - (\boldsymbol{\lambda}_r^T\boldsymbol{\lambda}_v/\lambda_v^2)\boldsymbol{\lambda}_v\right] \tag{A12}$$

$$\boldsymbol{S}_r^T = C_A\boldsymbol{Q}_r^T + C_Q\boldsymbol{A}_r^T + (\boldsymbol{\lambda}_v^T/\boldsymbol{\lambda}_v)[M_r] \tag{A13}$$

$$\boldsymbol{S}_v^T = C_A\boldsymbol{Q}_v^T + C_Q\boldsymbol{A}_v^T + (\boldsymbol{\lambda}_v^T/\boldsymbol{\lambda}_v)[M_v] \tag{A14}$$

$$\boldsymbol{S}_\lambda^T = C_Q\boldsymbol{A}_\lambda^T + (\boldsymbol{\lambda}_v^T/\boldsymbol{\lambda}_v)[M_\lambda] + (A_F/\lambda_v)\left[\boldsymbol{Q}_v^T - B_Q(\boldsymbol{\lambda}_v^T/\boldsymbol{\lambda}_v)\right] + (q/\lambda_v)\left[\boldsymbol{A}_v^T - B_A(\boldsymbol{\lambda}_v^T/\boldsymbol{\lambda}_v)\right] \tag{A15}$$

$$S_T = (1/m)\Big\{\left[(C_A + A_F/c)\boldsymbol{Q}_v^T + (C_Q + q/c)\boldsymbol{A}_v^T + (\boldsymbol{\lambda}_v^T/\boldsymbol{\lambda}_v)[M_v]\right](\boldsymbol{\lambda}_v/\lambda_v) + (qA_F/c^2)\Big\} \tag{A16}$$

By nulling $\ddot{S}_F$, it is easy to obtain the optimal thrust magnitude T^* during the singular arc:

$$T^* = (m\Lambda/S - \boldsymbol{S}_r^T\boldsymbol{v} - \boldsymbol{S}_v^T\boldsymbol{a}_0 - \boldsymbol{S}_\lambda^T\boldsymbol{\lambda}_v)/S_T \tag{A17}$$

One should note that Eqs. (A13–A16) vanish in the absence of aerodynamic terms; consequently, the denominator of Eq. (A17), also vanishes thus justifying the exclusion of singular arcs outside the atmosphere.

Acknowledgment

This research has been supported by the Agenzia Spaziale Italiana.

References

[1]Mease, K. D., "Optimization of Aeroassisted Orbital Transfer: Current Status," *Journal of the Astronautical Sciences*, Vol. 36, Nos. 1/2, 1988, pp. 7–33.

[2]London, H. S., "Change of Satellite Orbit Plane by Aerodynamic Maneuvering," *Journal of the Aerospace Sciences*, Vol. 29, No. 3, 1962, pp. 323–332.

[3]Miele, A., "Recent Advances in the Optimization and Guidance of Aeroassisted Orbital Transfers," International Astronautical Federation, Paper IAF 94 A.2.010, Oct. 1994.

[4]Miele, A., Basapur, V. K., and Lee, W. Y., "Optimal Trajectories for Aeroassisted, Noncoplanar Orbital Transfer," *Acta Astronautica*, Vol. 15, Nos. 6/7, 1987, pp. 399–411.

[5]Vinh, N. X., and Hanson, J. M., "Optimal Aeroassisted Return from High Earth Orbit with Plane Change," *Acta Astronautica*, Vol. 12, No. 1, 1985, pp. 11–25.

[6]Calise, A. J., "Singular Perturbation Analysis of the Atmospheric Orbital Plane Change Problem," *Journal of the Astronautical Sciences*, Vol. 36, Nos. 1/2, 1988, pp. 35–44.

[7]Casalino, L., Colasurdo, G., and Pastrone, D., "Indirect Approach for Minimum-Fuel Aeroassisted Transfers," *Proceedings of the AIAA/AAS Astrodynamic Conference*, AIAA, Reston, VA, 1996, pp. 192–200.

[8]Colasurdo, G., and Pastrone, D., "Indirect Optimization Method for Impulsive Transfer," *Proceedings of the AIAA/AAS Astrodynamics Conference*, AIAA, Washington, DC, 1994, pp. 441–448.

[9]Mease, K. D., Lee, W. Y., and Vinh, N. X., "Orbital Changes During Hypersonic Aerocruise," *Journal of the Astronautical Sciences*, Vol. 36, Nos. 1/2, 1988, pp. 103–137.

[10]Mease, K. D., Vinh, N. X., and Kuo, S. H., "Optimal Plane Change During Constant Altitude Hypersonic Flight," *Journal of Guidance, Control, and Dynamics*, Vol. 14, No. 4, 1991, pp. 797–806.

[11]Madepalli, S., and Vinh, N. X., "Optimal Plane Change of an Elliptic Orbit During Aerocruise," *Journal of the Astronautical Sciences*, Vol. 40, No. 4, 1992, pp. 503–525.

[12]Ross, I. M., "Extremal Angle of Attack over a Singular Thrust Arc in Rocket Flight," *Journal of Guidance, Control, and Dynamics*, Vol. 20, No. 2, 1997, pp. 391–393.

[13]Casalino, L., Colasurdo, G., and Pastrone, D., "Optimal Aeroassisted GEO-to-LEO Transfer by an Indirect Method," *Advances in the Astronautical Sciences*, Vol. 90, Univelt, Inc., San Diego, CA, 1995, pp. 2147–2161.

[14]Lawden, D. F., *Optimal Trajectories for Space Navigation*, Butterworths, London, 1963, pp. 54–68.

[15]Vinh, N. X., "General Theory of Optimal Trajectories for Rocket Flight in a Resisting Medium," *Journal of Optimization Theory and Applications*, Vol. 11, No. 2, 1973, pp. 189–202.

[16]Casalino, L., Colasurdo, G., and Pastrone, D., "Optimization Procedure for Preliminary Design of Opposition-Class Mars Missions," *Journal of Guidance, Control, and Dynamics*, Vol. 21, No. 1, 1998, pp. 134–140.

[17]Bryson, A. E., and Ho, Y. C., *Applied Optimal Control*, (rev.) Hemisphere, Washington, DC, 1975, pp. 90–127.

[18]Mease, K. D., and Vinh, N. X., "Minimum-Fuel Aeroassisted Orbit Transfer Using Lift Modulation," *Journal of Guidance, Control, and Dynamics*, Vol. 8, No. 1, 1985, pp. 134–141.

[19]Casalino, L., "Energetic Optimization of Aeroassisted Orbital Maneuvers," Ph.D. Dissertation, Dipartimento di Energetica, Politecnico di Torino, Turin, Italy, Feb. 1997, pp. 106–128 (in Italian).